Engineering Notes

Analytical Criterion for Aircraft Spin Susceptibility

A. A. Paranjape*
University of Illinois at Urbana-Champaign, Urbana, Illinois 61801
and
N. Ananthkrishnan[†]
Korea Advanced Institute of Science and Technology, Daejeon 305-701, Republic of Korea

I. Introduction

AIRCRAFT spin is mysterious, exciting, dangerous, and perhaps the biggest unsolved problem in flight mechanics. Spin is a critical phenomenon for both military and general aviation airplanes, and hence a matter of concern to aircraft designers and flight test engineers. Abzug and Larrabee [1] provide an instructive account of the history of spin research. Traditionally, spin onset was viewed as an instability problem along the lines of wing rock, yaw departure, nose slice and others of that ilk, leading to criteria for spin susceptibility of aircraft configurations, such as the widely used Weissman criterion [2]. Also of interest was the prediction of equilibrium spin characteristics (yaw rate r, angle of attack α, etc.) and identifying control combinations favoring entry into spin and recovery from spin, typically using approximate methods and reduced-order models [3,4]. However, with the introduction of bifurcation methods and the use of continuation algorithms, it became possible to work with the complete set of aircraft equations of motion with no approximation, and to numerically compute all steady states and identify all points of instability onset [5,6]. It became clear that spin was primarily a high-α steady state with large angular rates which could itself be either stable or unstable. Entry into spin was typically found to occur by way of a jump phenomenon due to onset of an instability on a coexisting low-α branch of steady states [7]. The nature of the spin (steady or oscillatory, erect or inverted, flat or steep, left- or right-hand) could be predicted from a bifurcation analysis and strategies to recover from spin could be worked out [8].

To clarify, consider the schematic bifurcation diagram sketched in Fig. 1, which presents two possible spin entry scenarios. In each case, there is a single branch of steady states that folds over twice to give a stable high-α branch representing spin states. Entry into spin in both the diagrams is through a jump phenomenon marked on the diagrams by a vertical up-arrow. The point of onset of jump in each part figure is at an instability on the low-α stable branch or a branch derived from it. For instance, in Fig. 1a, the low-α branch retains its stability till the first foldover point, called a saddle-node bifurcation (SNB); when the elevator deflection is decreased beyond this point, entry into spin

occurs by way of a jump. Such a jump phenomenon is common, for example, in rapid rolling maneuvers leading to possible autorotation [9]. Whereas in Fig. 1b, the low-α branch becomes unstable part way at a Hopf bifurcation (HB) where a stable branch of limit cycles is created which then folds over at a fold bifurcation (FB) to yield unstable limit cycles and a jump entry to spin. Such a sequence (HB followed by FB) is akin to what is observed in case of aircraft wing rock [10].

The existence of a high-α (and large yaw rate) stable spin branch which arises from the second SNB point is common to both scenarios. Furthermore, there is a clear point of spin onset (the first SNB point in Fig. 1a and the FB point in Fig. 1b) which could correspond to a standard instability (yaw departure, wing rock onset, stall, etc.) of the primary (low-α) branch of steady states. In such cases, traditional spin onset criteria, such as the Weissman criterion, are often successful.

However, other variants of the basic scenarios in Fig. 1 are possible, for example, the high-α spin branch may be unstable, or the instability on the low-α branch may either not yield a jump to spin or may lead to a high-α phenomenon other than spin. In these cases, the traditional spin onset criteria are not applicable, nor is it helpful to seek stable spin equilibria. To illustrate this, Fig. 2 shows a concrete example of the bifurcation diagram for the F-18 high-alpha research vehicle (HARV) reproduced from [8]. The primary steady state branch shows increasing-α trims with up-elevator before finally losing stability at a Hopf bifurcation (H1) around $\alpha = 0.75$ rad (43 deg). It then continues unstable but less steeply due to reduced elevator effectiveness at the higher α until the up-elevator limit is reached at $\alpha = 1.0$ rad. When continued further beyond the limit, the unstable branch folds over and still unstable, reenters the frame of the figure. It runs up to 1.2 rad angle of attack, where it folds over a second time to give the high-α spin branch with large negative yaw rates. Note that in this case the first SNB point is outside the physical range of elevator deflection values, hence cannot be a point of instability for spin onset. The high-α spin equilibrium branch (dashed line running left beyond 1.2 rad angle of attack and -1.4 rad/s yaw rate) is unstable but the Hopf bifurcation (H2) gives a branch of stable spin limit cycles (filled circles). Interestingly, the instability at 0.6 rad (35 deg) angle of attack is stall, but this does not lead to spin as, at that elevator deflection, there is no equilibrium spin branch to jump to. Also, the instability at the Hopf bifurcation point (H1) causes a jump to the pitch bucking limit cycles which originate at the Fold bifurcation point (F1), and not to spin. Simulations show that, for this particular airplane, it is apparently impossible to enter spin from a straight wings-level flight by merely pitching the nose up; however, entry into spin is possible from a low-α descending turn by using a rapid pitch up [11].

Thus, traditional spin onset criteria may not always provide a good indicator to the spin susceptibility of a given configuration. Instead, it makes sense to evaluate the spin susceptibility of an aircraft by looking for the existence of high-α, high-angular-rate steady states, as in Figs. 1 and 2, regardless of their stability. The presence of unstable spin equilibria merely implies that the spin dynamics is more complicated, perhaps a limit cycle or even chaotic. Given such a spin state, the existence of some instability or the other, and a combination of control inputs, that results in jump to that spin state may be expected. Conversely, in the absence of such a spin state, the aircraft may be ruled as not susceptible to spin.

The existence of a high-α equilibrium spin branch can be deduced from the occurrence of the second SNB at high-α, as seen in the bifurcation diagrams in Figs. 1 and 2. While a numerical condition for the occurrence of the SNB may be easily obtained, an analytical criterion for spin susceptibility would not only give physical insight but also provide aircraft designers with a useful tool. Bifurcation

*Doctoral Candidate, Department of Aerospace Engineering; paranja2@illinois.edu. Student Member AIAA.
†Research Professor, Division of Aerospace Engineering, KAIST, 373-1 Guseong-dong, Yuseong-gu; drakn19@kaist.ac.kr. Associate Fellow AIAA.
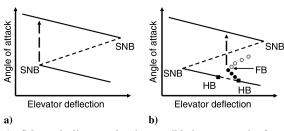
Fig. 1 Schematic diagram showing possible jump scenarios for entry into spin at a) a SNB, and b) at a FB of limit cycles (full line: stable trim; dashed line: unstable trim; filled circle: maximum amplitude of stable limit cycle, empty circle: maximum amplitude of unstable limit cycle, filled square: HB).

Fig. 2 Bifurcation diagram of F-18 HARV model from [8] showing high-α spin states at large negative yaw rates. The aileron and rudder were both set to zero, i.e., $\delta_a = \delta_r = 0$ (Full line: stable trim, Dashed line: unstable trim, Filled circle: maximum amplitude of stable limit cycle, Empty circle: maximum amplitude of unstable limit cycle, Filled square: Hopf bifurcation, Empty square: pitchfork bifurcation).
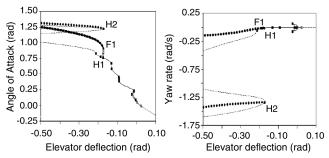
theory has been used in the past to derive approximate analytical criteria for instabilities such as wing rock [12] and roll-coupled instabilities [13]. The aim of the present work is to obtain an analytical criterion using bifurcation theory for spin susceptibility of an aircraft based on detecting the occurrence of the second SNB point.

Note that the intermediate branch of steady states, between the two SNB points in Figs. 1 and 2, despite being high-α, large-yaw-rate states, does not represent spin. This is because all equilibrium states on this branch carry an odd number of right-half-plane eigenvalues; hence they can neither be stable nor give rise to another stable spin state (such as a limit cycle). Also note that this approach differs from previous work (e.g., see [4]), which sought to solve for the spin equilibrium state itself; instead, our approach infers the existence of spin equilibria by solving for the SNB point, which allows us to obtain a compact criterion independent of the nature of the spin solution (stable or unstable, steady or unsteady).

II. Derivation of the Analytical Criterion

The first step is to identify a low-order model for the equilibrium spin states using the minimum number of state variables to ensure analytical tractability while retaining the essential physics of the spin phenomenon. This is essentially along the lines of previous work (e.g., [4]), but there is a significant difference. For our criterion, it is not necessary to solve for the equilibrium spin states *per se*, but only for the SNB point at the start of the spin equilibrium branch.

A previous survey [14] has shown that the sideslip angles in developed spin are negligible, and unless the airplane is in a steeply banked attitude, the pitch rate is quite small relative to the roll and yaw rates. Hence, it is reasonable to assume equilibrium values of sideslip and pitch rate, $\beta = 0$ and $q = 0$, leaving α, p, r as the three independent variables. Note that these assumptions are applied only to the SNB point at the start of the spin equilibrium branch, which can be thought of as an incipient spin solution.

Following the usual practice [5], the reduced-order model for equilibrium spin states is taken to consist of the three moment equations, as follows:

$$\dot{p} = L_0(\delta) + L_p(\alpha)p + L_r(\alpha)r \tag{1}$$

$$\dot{q} = Arp + M(\alpha) + M_{\delta e}\delta e \tag{2}$$

$$\dot{r} = N_0(\delta) + N_p(\alpha)p + N_r(\alpha)r \tag{3}$$

where $A = (I_z - I_x)/I_y$, δ is the vector of control inputs, δe is the elevator deflection, and the dimensional stability and control derivatives have their usual meanings [15], except that they are divided by the respective inertia term. The terms L_0, N_0 contain the contribution of the lateral control inputs, and effects due to asymmetry between the control effectiveness of the right and left elevators. (Henceforth, the α dependence of the lateral derivatives is not written explicitly, for convenience.)

The equilibrium spin states are obtained by setting the left-hand side of Eqs. (1–3) to zero. Let $\Delta = L_pN_r - N_pL_r$. Then, solving for p and r from Eqs. (1) and (3) gives:

$$p = \frac{L_rN_0 - N_rL_0}{\Delta}, \qquad r = \frac{N_pL_0 - L_pN_0}{\Delta} \tag{4}$$

Using Eq. (4) in Eq. (2), one obtains:

$$A(L_rN_0 - N_rL_0)(N_pL_0 - L_pN_0) + \Delta^2(M(\alpha) + M_{\delta e}\delta e) = 0 \tag{5}$$

which is a single consolidated trim equation. Given N_0, L_0 (for a certain choice of control δ), it gives the relation between steady state angle of attack α and elevator deflection δe; that is, an approximation to the graphical representation of steady states in a bifurcation diagram, as in Fig. 2a. However, the aim of this exercise is to identify the SNB point at the start of that spin branch, and the above analysis of spin equilibria is only a means to that end.

The condition for a steady state (i.e., a solution of Eq. (5)) to be an SNB point is given by:

$$\frac{\partial \delta_e}{\partial \alpha} = 0 \tag{6}$$

By differentiating the left-hand side of Eq. (5) with respect to α and setting the condition in Eq. (6), and eliminating δe by using Eq. (5), the following equation is readily obtained:

$$A[(L_{r,\alpha}N_0 - N_{r,\alpha}L_0)(N_pL_0 - L_pN_0) + (L_rN_0 - N_rL_0)(N_{p,\alpha}L_0$$
$$- L_{p,\alpha}N_0)] + \Delta^2 M_\alpha(\alpha) - 2A\frac{\Delta_\alpha}{\Delta}(L_rN_0 - N_rL_0)(N_pL_0$$
$$- L_pN_0) = 0 \tag{7}$$

where the subscript , α denotes the partial derivative with respect to α. For given L_0, N_0, Eq. (7) is a function of α alone. When the left-hand side of Eq. (7) is plotted as a function of α, the zero crossings indicate the presence of SNB points. Thus, the SNB condition in Eq. (7) serves as a criterion for spin susceptibility of an aircraft configuration. Note that the equilibrium condition, Eq. (5) has been embedded in Eq. (7), hence it need not be explicitly solved.

When applied to the F-18 aircraft model (data in [8]) for the same choice of δ as in Fig. 2, the plot of the SNB criterion in Eq. (7) appears as shown in Fig. 3. Two zero crossings are evident, and the second zero crossing matches very closely the SNB point in Fig. 2 at the start of the branch of spin states. The first zero crossing corresponds to the first SNB point (seen in Fig. 1), which happens to be outside the range of δe values in Fig. 2. As explained earlier, the branch starting at the first SNB point cannot yield a stable spin state. It is the second SNB point and the second zero crossing in Fig. 3 that is of interest. Remarkably, the simple analytical criterion in Eq. (7) is able to predict the occurrence of the second SNB point at high-α, and thus serves as a useful criterion for spin susceptibility.
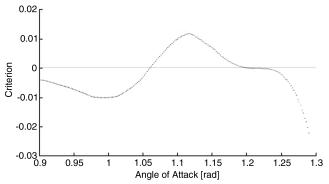
Fig. 3   Plot of the analytical criterion applied to the F-18 HARV model showing the SNB points corresponding to the zero crossings. The second zero crossing near 1.22 rad angle of attack is of interest for spin susceptibility.

III.   Another Form of the Criterion

The spin susceptibility criterion, Eq. (7), can be presented in an alternative, more graphical form, as follows. Using the following relations for L_0, N_0 obtained from Eqs. (1) and (3):

$$L_0 = -(L_p p + L_r r), \qquad N_0 = -(N_p p + N_r r) \qquad (8)$$

and replacing L_0, N_0 in Eq. (7) for the SNB criterion in terms of p, r as above, and using a further approximation, $p = r \cot \alpha$, gives

$$Ar^2[(L_{p,\alpha} N_p - N_{p,\alpha} L_p)\cot^2\alpha + (N_{r,\alpha} L_r - L_{r,\alpha} N_r) - \cot\alpha \Delta_\alpha]$$
$$+ \Delta M_\alpha(\alpha) = 0 \qquad (9)$$

where $\Delta = L_p N_r - N_p L_r$ as before. This version of the SNB criterion only requires the following aerodynamic parameters as functions of α: L_p, L_r, N_p, N_r, M_α. Notably, Eq. (9) is a single equation in two variables, α and r, for the SNB points. Thus, it can be solved to give the trace of all SNB points in two-dimensional $r - \alpha$ space. Of these, we need to select the SNB point that corresponds to the start of the spin equilibria branch. This contrasts with the previous form of the criterion where, among all spin equilibria, we find the one with the special property of being an SNB point. In this alternative form, among all SNB points, we wish to isolate the one with the special property of being a spin state (at least, the starting point of a branch of spin steady states).

A nice way to do this is to obtain the accessible region plot, which gives all possible equilibrium states at which the aircraft may be trimmed (balance of moments about all three axes) subject to availability of control. As suggested in [7], the accessible region may be computed by solving the trim moment equations in the form below:

$$C_l = 0; \qquad \frac{\overline{q}Sc}{I_y}C_m = -\frac{I_z - I_x}{I_y}r^2 \cot\alpha; \qquad C_n = 0 \qquad (10)$$

For the F-18 HARV data considered in this work, superimposing the set of SNB points from Eq. (9) and the accessible region trims from Eq. (10), yields the plot in Fig. 4. The patch of filled diamonds in Fig. 4 is the accessible region in $r - \alpha$ space, whereas the set of SNB points is marked by open circles. This composite plot is interesting because the accessible region is restricted by control deflection limits while the SNB points are not, but on the other hand the accessible region does not distinguish between stable and unstable trims while the SNB points are all neutrally stable (having one zero eigenvalue). Hence, one should only consider points that lie at the intersection of the SNB plot and the accessible region in Fig. 4, of which there are three sets.

At negative yaw rates, there is a connected path through the accessible region that intersects the SNB locus twice: first around $\alpha = 1.05$ rad, and a second time near $\alpha = 1.22$ rad. These intersections correspond to the zero crossings in Fig. 3, while only the second crossing is seen in Fig. 2. Thus, Fig. 4 predicts a set of left spin
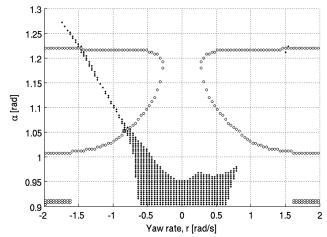

Fig. 4   Composite plot of SNB points from Eq. (9) marked by open circles and the accessible region from Eq. (10) plotted with filled diamonds. The gray square is the first SNB point not seen in Fig. 2 and corresponds to the first zero crossing in Fig. 3.

states originating at the second SNB intersection, which corresponds closely to what is observed in numerical studies and spin tunnel tests [16]. However, Fig. 4, in a concise manner, carries more information than what is available in the plot of the analytical criterion in Fig. 3. Besides an additional axis for the yaw rate, which allows one to judge the nature (left or right) of the spin state emerging at the second SNB point, the accessible region in Fig. 4 considers limits on all the control deflections simultaneously. Thus, for example, the first SNB point at $\alpha \approx 1.05$ rad, which lies outside the range of δe limits for the chosen values of the lateral control inputs in Fig. 2, is seen in Fig. 4 (gray square) to be inaccessible, but the first SNB points for other sets of control deflection are accessible. More important, Fig. 4 reveals unconnected, accessible, high-α, large-yaw-rate SNB points, such as the intersection at $\alpha = 1.22$ rad and positive yaw rate. This third intersection set suggests the possibility of right spin states, but these have yet to be confirmed.

IV.   Conclusions

This paper presents an analytical criterion for spin susceptibility of airplanes based on the occurrence of a second SNB point at high angles of attack and large yaw rates signifying incipient spin. This approach is a significant departure from previous ones, which focused on either identifying low-α instabilities that may lead to spin onset or on explicitly seeking spin equilibria. Consequently, the analytical criterion could be obtained in a simple form, which is presented in two complementary ways: one, in terms of the zeros of a simple algebraic expression as a function of angle of attack, and alternatively as a composite plot of SNB points and accessible regions in $r - \alpha$ space. The composite plot simultaneously considers limits on all control deflections, identifies unconnected SNB points, and is likely to be more useful to the designer. The prediction by either form of the criterion is seen to match extremely well with spin onset observed in computations and in the spin tunnel for the F-18 HARV. The criterion needs to be tested against further sets of aircraft data; nevertheless, the present results are a significant achievement for the complex, longstanding and formidable problem of aircraft spin.

References

[1] Abzug, M. J., and Larrabee, E. E., *Airplane Stability and Control: A History of the Technologies that Made Aviation Possible*, Cambridge Univ. Press, Cambridge, England, 1997, pp. 115–139.

[2] Weissman, R., "Status of Design Criteria for Predicting Departure Characteristics and Spin Susceptibility," *Journal of Aircraft*, Vol. 12, No. 12, 1975, pp. 989–993.
doi:10.2514/3.59904

[3] Tischler, M. B., and Barlow, J. B., "Determination of the Spin and Recovery Characteristics of a General Aviation Design," *Journal of Aircraft*, Vol. 18, No. 4, 1981, pp. 238–244.
doi:10.2514/3.57487

[4] Bihrle, W., Jr., and Barnhart, B., "Spin Prediction Techniques," *Journal of Aircraft*, Vol. 20, No. 2, 1983, pp. 97–101.
doi:10.2514/3.44837

[5] Goman, M. G., Zagaynov, G. I., and Khramtovsky, A. V., "Application of Bifurcation Theory to Nonlinear Flight Dynamics Problems," *Progress in Aerospace Sciences*, Vol. 33, No. 9, 1997, pp. 539–586.
doi:10.1016/S0376-0421(97)00001-8

[6] Paranjape, A. A., Sinha, N. K., and Ananthkrishnan, N., "Use of Bifurcation and Continuation Methods for Aircraft Trim and Stability Analysis: A State-of-the-Art," *Journal of Aerospace Sciences and Technologies*, Vol. 60, No. 2, 2008, pp. 1–16.

[7] Goman, M. G., Khramtovsky, A. V., and Kolesnikov, E. H., "Evaluation of Aircraft Performance and Maneuverability by Computation of Attainable Equilibrium Sets," *Journal of Guidance, Control and Dynamics*, Vol. 31, No. 2, 2008, pp. 329–339.
doi:10.2514/1.29336

[8] Raghavendra, P. K., Sahai, T., Kumar, P. A., Chauhan, M., and Ananthkrishnan, N., "Aircraft Spin Recovery, with and without Thrust Vectoring, using Nonlinear Dynamic Inversion," *Journal of Aircraft*, Vol. 42, No. 6, 2005, pp. 1492–1503.
doi:10.2514/1.12252

[9] Ananthkrishnan, N., and Sudhakar, K., "Prevention of Jump in Inertia-coupled Roll Maneuvers of Aircraft," *Journal of Aircraft*, Vol. 31, No. 4, 1994, pp. 981–983.
doi:10.2514/3.46591

[10] Ananthkrishnan, N., and Sudhakar, K., "Characterization of Periodic Motions in Aircraft Lateral Dynamics," *Journal of Guidance, Control and Dynamics*, Vol. 19, No. 3, 1996, pp. 680–685.
doi:10.2514/3.21674

[11] Ghosh, K., "Effect of Thrust Vectoring on Aircraft Trim, Stability, and Maneuvers," Masters Dissertation, Department of Aerospace Engineering, Indian Inst. of Technology Bombay, Mumbai, India, May 2006.

[12] Ananthkrishnan, N., Shah, P., and Unnikrishnan, S., "Approximate Analytical Criterion for Aircraft Wing Rock Onset," *Journal of Guidance, Control and Dynamics*, Vol. 27, No. 2, 2004, pp. 304–307.
doi:10.2514/1.2975

[13] Mahale, A., and Ananthkrishnan, N., "Analytical Criterion for Onset of Departure in Inertia-coupled Roll Maneuvers of Airplanes," AIAA Paper AIAA-2006-6267, 2006.

[14] Chambers, J. R., and Grafton, S. B., "Aerodynamic Characteristics of Airplanes at High Angles of Attack," NASA TM 74097, Dec. 1977.

[15] Etkin, B. E., and Reid, L. D., *Dynamics of Flight: Stability and Control*, 3rd ed., Wiley, New York, 1996, pp. 118–120.

[16] Fremaux, C. M., "Spin Tunnel Investigation of a 1/28-Scale Model of the NASA F-18 High Alpha Research Vehicle (HARV) with and Without Vertical Tails," NASA CR-201687, Apr. 1997.